Spectroscopy of quasi-particle scattering in superconductors

Z. Janů, M. Novák, F. Soukup, R. Tichý, G.M. Tsoi

Joint Low Temperature Laboratory (IP ASCR&FMF ChU), Prague, Czech Republic

Samples:
A. Bondarenko, TU Kharkov, Ukraine
M. Gaiffulin, U Tokyo, Japan
X.L. Wang TU Linz, Austria
V. Buntar, AI Wien, Austria

Motivation

- S-N transition close T_c, with $\delta T \sim 1$ mK and almost single vortex resolution on high-quality single crystals or epitaxial films
- Vortex matter phases diagram close T_c
- $M(T)$ — S-N transition
- $M(H)$, $H_{c1}(T)$, and $H_{c2}(T)$ — magnetization curves, phase diagram
- $M(t)$ — flux relaxation with ms resolution

Domain non accessible by commercial magnetometers

High Resolution SQUID Magnetometer

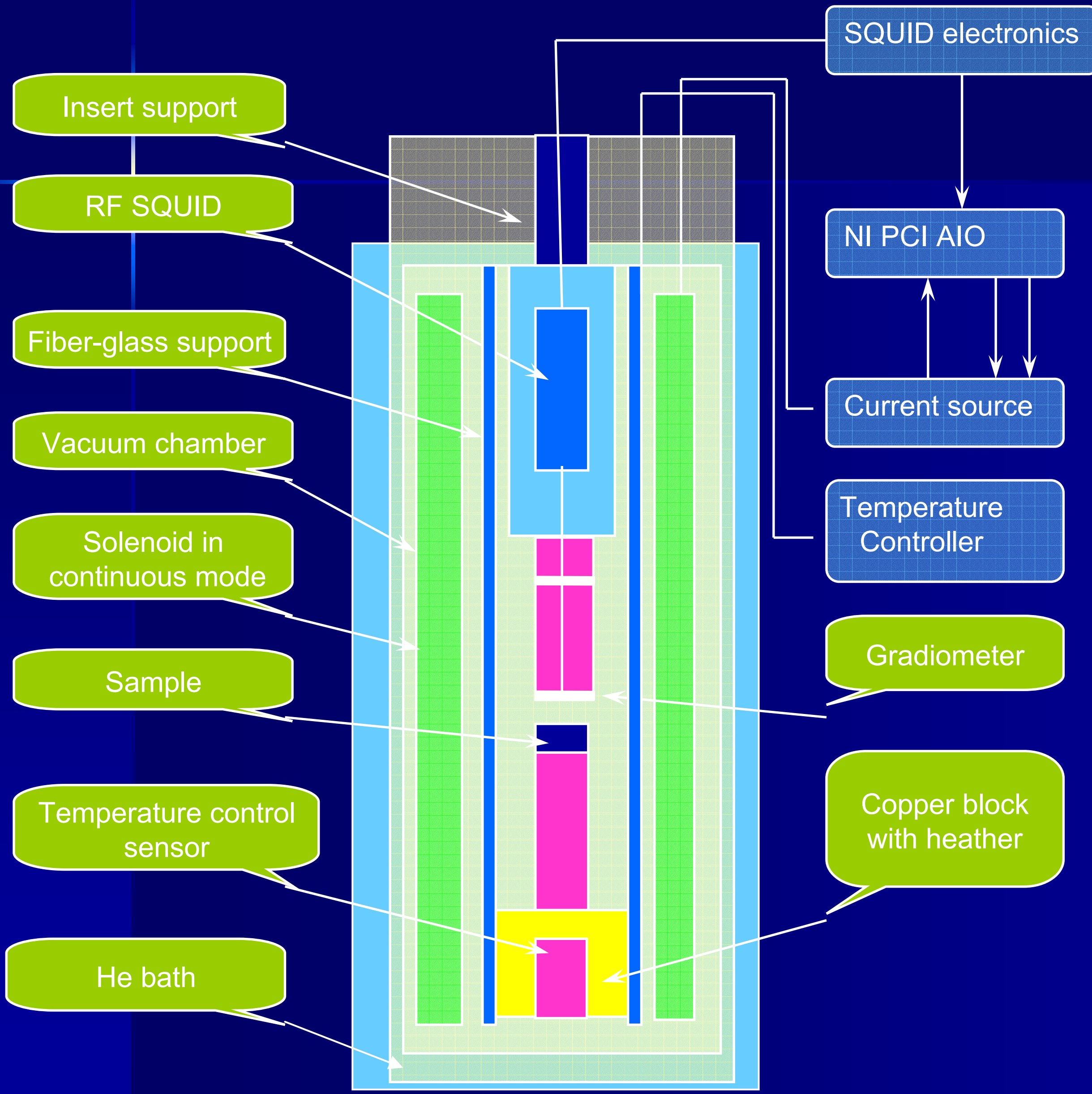

Sample stationary both with respect to the solenoid and detection system

Field range (ac&dc) < 138 μT

Residual noise ~1 nT

Frequency range 0.01-10 Hz

Temperature range 4.2-150 K

Temperature stability and resolution 1 mK

OUT:AWG: applied field (dc&ac)

IN: $H(t)$ [V], $\Phi(t)$ [V] => FFT =>H(f), $\Phi(f)$,

f from dc to 2 kHz

Contact-less bulk measurement

- Shielding current *I* is induced in the sample by applied field *H*

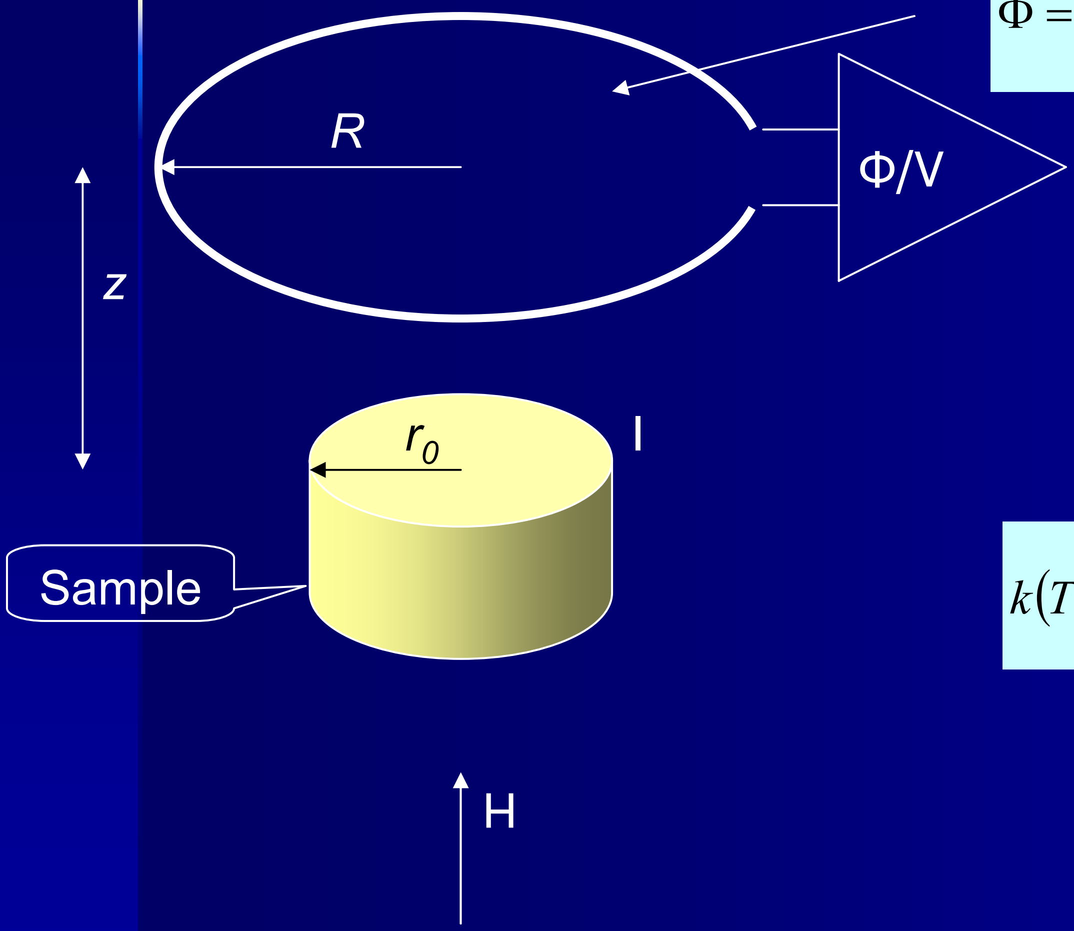

$$\Phi = \int_0^{r_0} A_\varphi(r)\sqrt{\frac{R}{r}}\left[\left(\frac{2}{\eta}-\eta\right)\mathrm{K}(\eta)-\frac{2}{\eta}\mathrm{E}(\eta)\right]\mathrm{d}\,r$$

$$\eta^2 = 4rR/\left[(r+R)^2+z^2\right]$$

$$A_\varphi(r) = A_\varphi(r_0)\mathrm{K}_0(k(r_0-r))/\mathrm{K}_0(kr_0)$$

$$k(T) = \frac{1}{\lambda(T)} = \sqrt{\mu_0\frac{e^2 n_s(T)}{m}} \propto \sqrt{1-(T/T_c)^\alpha}$$

YBCO single crystal in H||*c* and H||*ab*

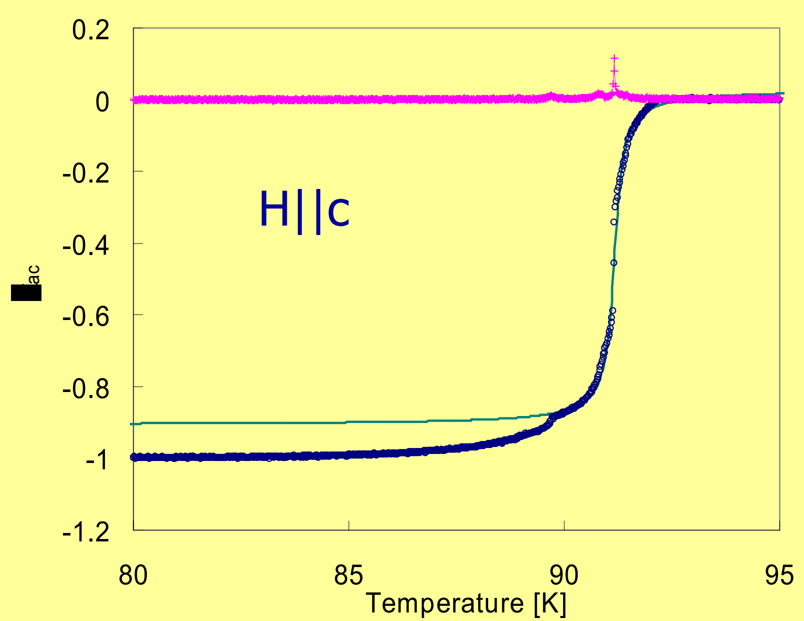

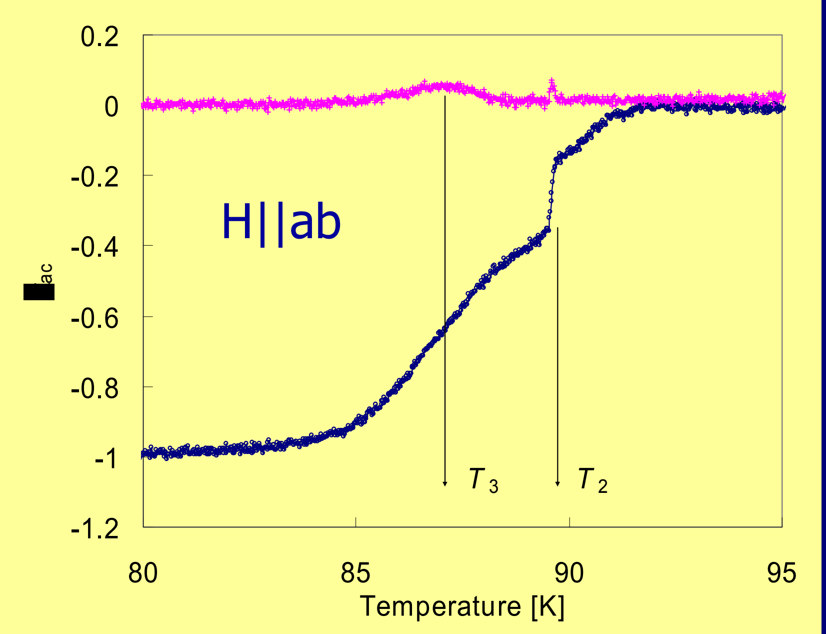

The T_1 transition occurs in *ab* plane, while T_2 and T_3 transitions occur in *c*-axis direction. The T_1 transition shows appearance of 2D superconductivity in CuO_2 layers. Below T_2 become superconducting CuO_2-Y-CuO_2 bi-layers. Above T_2 the Y layers are in normal state while SNS sandwiches become superconducting due to a proximity effect. In **H**||*c* this transitions is masked by superconducting CuO_2 layers. Finally, below T_3 the CuO_2-Y-CuO_2 sandwiches become weakly coupled and super-current tunnels through the Ba-CuO-Ba barriers. At even lower temperature the superconductivity is 3D.

Janu Z. *et al.*, Physica C **388-9** (2003) 751

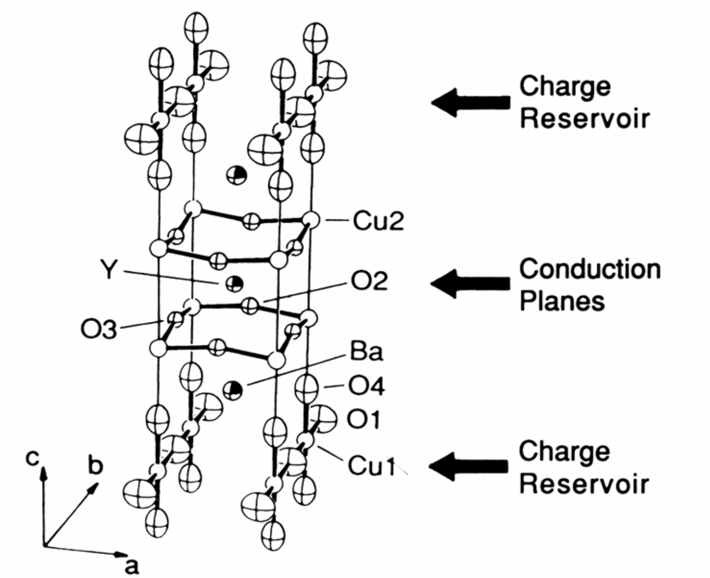

Fig. 1. Structure of $YBa_2Cu_3O_{6+x}$ showing the charge reservoir and conduction plane regions associated with the charge transfer model.

The real part is bl… one is read.

Superconducting multilayers with different T_c

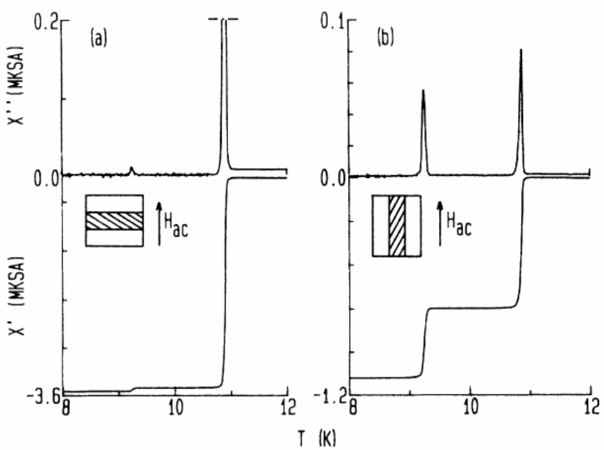

FIG. 5. Simulation of the screening effect with NbTi plate sandwiched between two NbZr plates. (a) h_{ac} (1 Oe) perpendicular to the plates. The signal $\Delta X'$ corresponding to the transition of NbTi plate is around 1.8% of the whole transition. (b) For H_{ac} (0.1 Oe) parallel to the plates the transition of NbTi is around the expected value of 36% (no screening effect in this case).

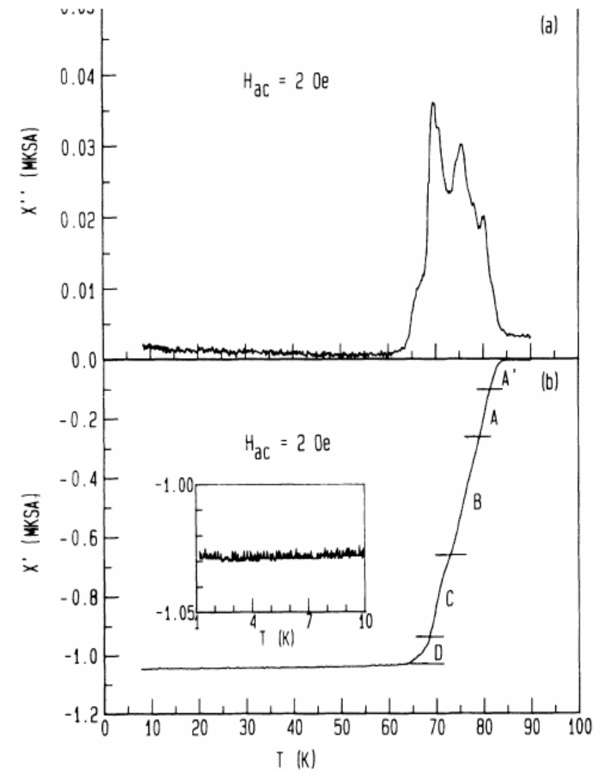

FIG. 1. $X''(T)$ and $X'(T)$ for H_{ac} (2 Oe) parallel to the *ab* basal plane show different superconducting phases *A'*, *A*, *B*, *C*, *D*. The inset shows the $X'(T)$ variation at low temperature.

YBCO in H||c

- Ac field dependence

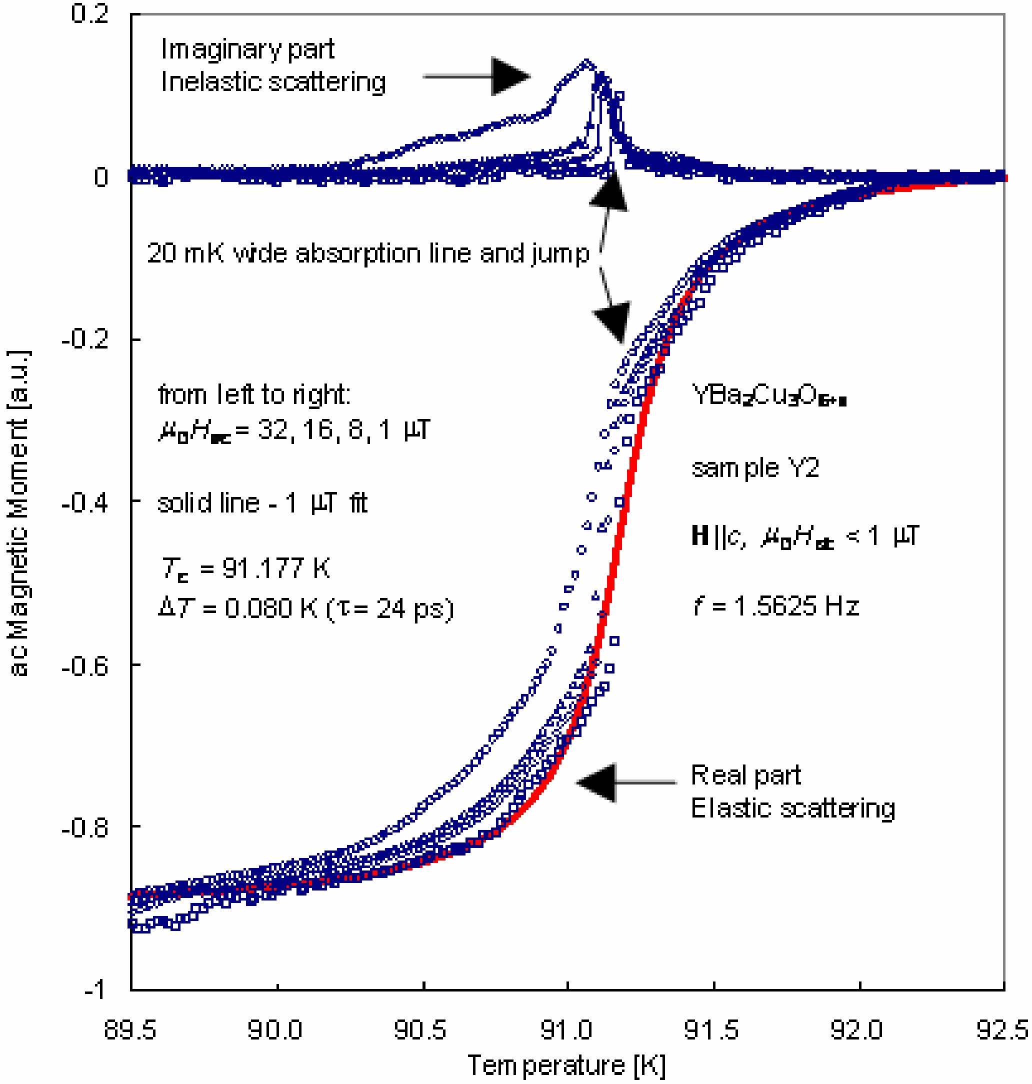

”Universal” behavior of YBCO and BSCCO

Y2: 0.29x1.725 mm², 35 μm thickness

H||c, $\mu_0 H_{ac}$ = 1 μT, $\mu_0 H_{dc}$ = 0 μT,

f = 1.5625 Hz

B17A: 700x840 μm², 40 μm thickness

H||c, $\mu_0 H_{ac}$ = 300 nT, $\mu_0 H_{dc}$ = 50 μT,

f = 1.5625 Hz

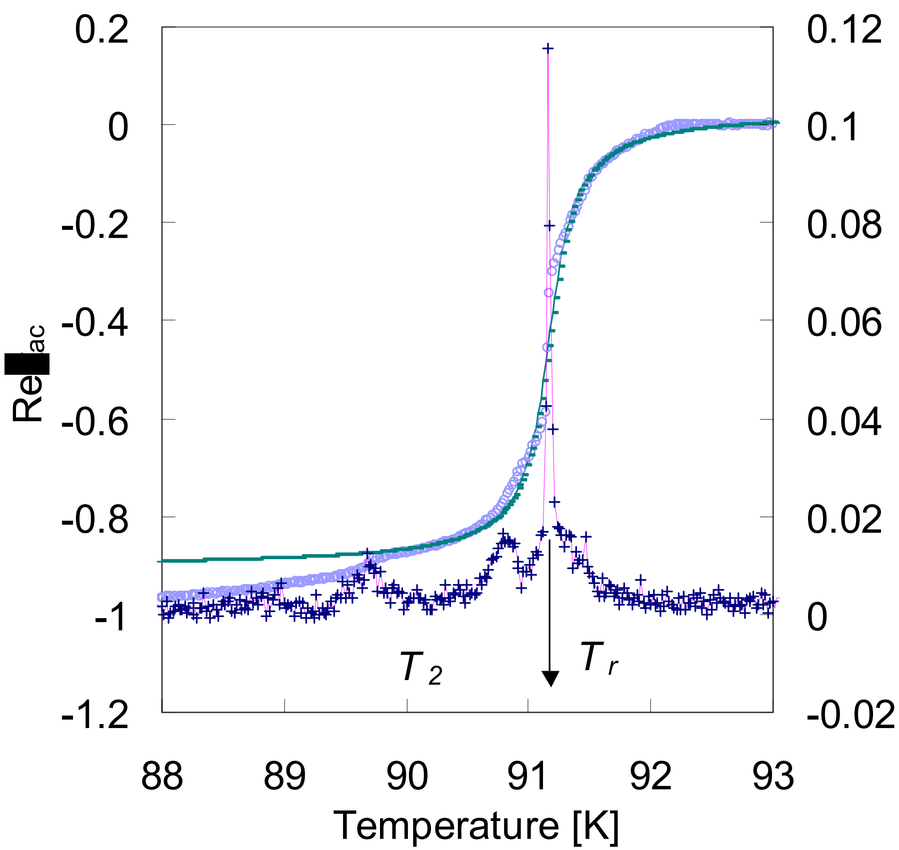

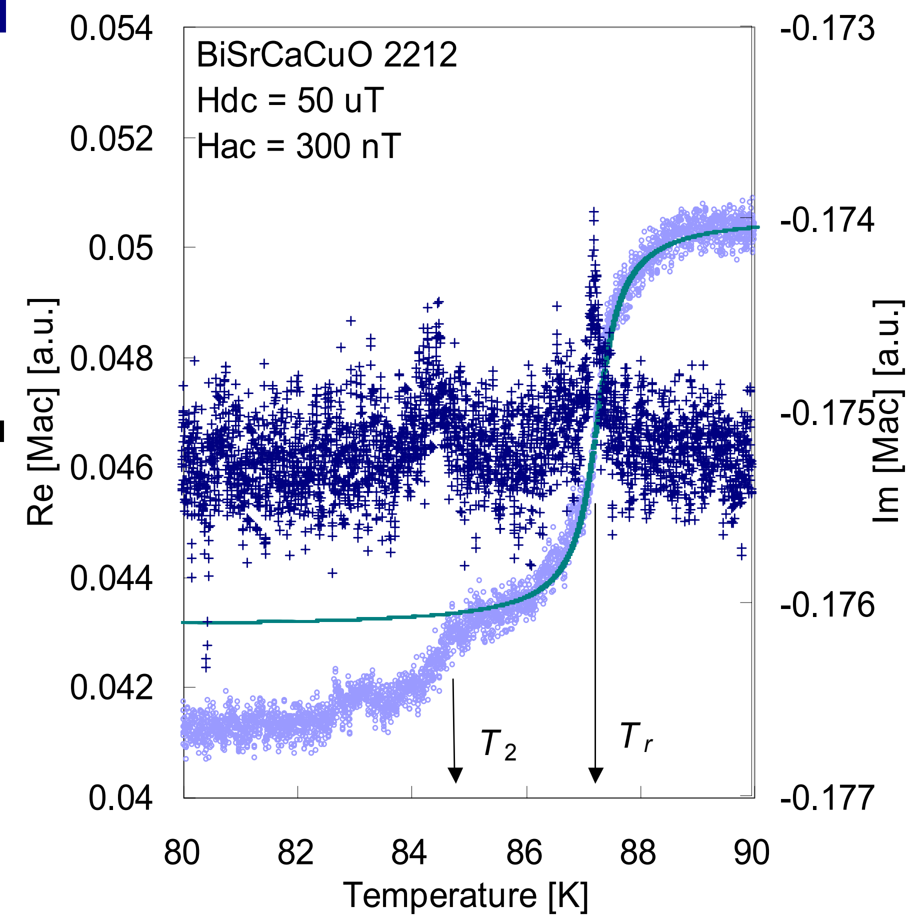

Problems:

Standard models explain the temperature dependence of the susceptibility due to a flux penetration length, which depends on the superfluid density:

Two fluid Casimir-Gorter model: $n_s(T) \sim 1 - (T/T_c)^4$

Ginzburg-Landau model: $n_s(T) \sim 1 - (T/T_c)$

BCS - close to T_c like GL

- These models fail to describe very slow decrease of $\mathrm{Re}\chi_{ac}(T)$ far below T_c and too fast near T_c. Approximation with temperature dependent superfluid density gives unrealistic parameters (exponents).
- Nonvanishing absorption ($\mathrm{Im}\chi_{ac}(T)$) for $H_{ac} \rightarrow 0$ shows that the transition is first-order.
- Phase transition in vortex matter? The temperature of vortex lattice melting should depend on H_{dc} (vortex density) and frequency of H_{ac}. But no dependence is observed.
- *S*-shaped $\mathrm{Re}\chi_{ac}(T)$ and 10 mK narrow line on $\mathrm{Im}\chi_{ac}(T)$? This cannot be due to a fluctuations above T_c.

- What is wrong?
- Data fit simple function

$$\mathrm{Re}\,\chi(T) = a + b\arctan\frac{2(T - T_c)}{\Delta T_c}$$

This dependence is known as **Breit-Wigner resonance**:

- Analogy with resonances in optics, here for particle waves

Breit-Wigner resonance in solids

- Isolated resonance level
- Electrons in Fabry-Perrot resonator with R->1
- Coupled channel resonance
- Two near continua
- Auto-ionization
- Hybridization (n-merization)

Not super-fluid density but electron scattering

- Total current = paramagnetic + diamagnetic [BCS]
- Paramagnetic (*T* dependent) = quasi-particle current = counter-flow
- Diamagnetic (*T* independent) = all conduction electrons = solid state – single wave function
- Linear response of current density to vector potential = ideal diamagnetism
- There has to be correlated electrons

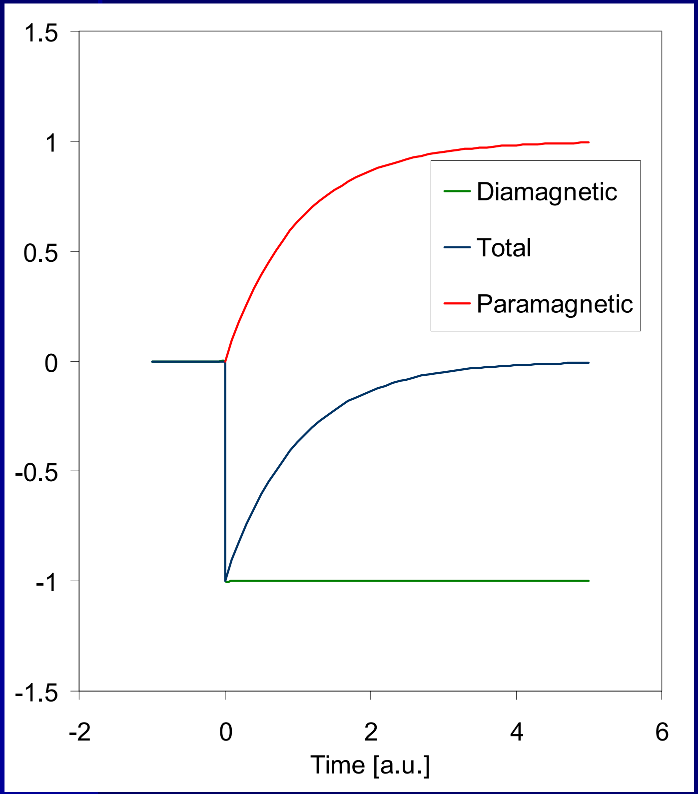

$$\mathbf{j} = \frac{en}{m}\left(\hbar\mathbf{k} - e\mathbf{A}\right)$$

$$\mathbf{K} = \sum_{\mathbf{k}} \mathbf{k} c^{*}_{\mathbf{k}-\mathbf{K}} c_{\mathbf{k}}$$

$$\mathbf{J} = \frac{en}{m}\left(\hbar\mathbf{K} - e\mathbf{A}\right) = i\sigma\omega\mathbf{A}$$

$$\mathbf{M} = \frac{en}{m}\left(\hbar\oint_{\Gamma}\mathbf{K}\,d\mathbf{l} - e\Phi\right) = i\omega\sigma\Phi$$

$$\mathbf{M} = \frac{en_0}{m}\left(\hbar\oint_{\Gamma}\nabla\phi\,d\mathbf{l} - e\Phi\right)$$

$$\Psi = \Psi_0 \exp\left(i\phi\right)$$

- Temperature dependent paramagnetic (drift, counter-flow) current
- Temperature independent diamagnetic current of all conduction electrons of both spin direction, which has the same value both in the normal and superconducting states

$$\mathbf{j}(T) = \frac{ne}{m} \hbar \mathbf{K}(T)$$

$$\mathbf{j} = -\frac{ne^2}{m} \mathbf{A}$$

Magnetization: $$\mathbf{M}(T) = \frac{ne}{m} \left[\hbar \oint_{\Gamma} \mathbf{K}(T) \cdot d\mathbf{l} - e\Phi \right]$$

K is the complex wave-vector – temperature dependent

Real part - elastic electron scattering (non-Ohmic)

Imaginary part - inelastic electron scattering (Ohmic)

Electron scattering

BCS:

•Copper pairs

•low angle forward isotropic scattering from longitudinal phonons

$$\left|\mathbf{k}\uparrow\right\rangle+\left|-\mathbf{k}\downarrow\right\rangle=\left|\mathbf{K}\uparrow\downarrow\right\rangle, \Delta K\xi \geq 1/2$$

$$\mathbf{k}_{\uparrow} \rightarrow \mathbf{k}_{\uparrow}+\mathbf{q}$$
$$-\mathbf{k}_{\downarrow} \rightarrow -\mathbf{k}_{\downarrow}-\mathbf{q}$$

Back-scattering from (super)lattice

In 1970s: Gorkov – A15 – have superstructure

Scalapino – analogy of Peierls instability in 1D with BCS

Low dimensional systems

$$\mathbf{k} \rightarrow \mathbf{k}-\mathbf{G}=-\mathbf{k}$$
$$-\mathbf{k} \rightarrow -\mathbf{k}+\mathbf{G}=\mathbf{k}$$

$$2\mathbf{k} \approx \mathbf{G}$$

We need further information on lattice and Fermi level – diffraction, ARPES, STM, ..

Fermi surface

- 3D
- 2D
- 1D

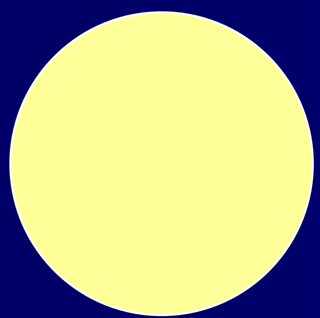

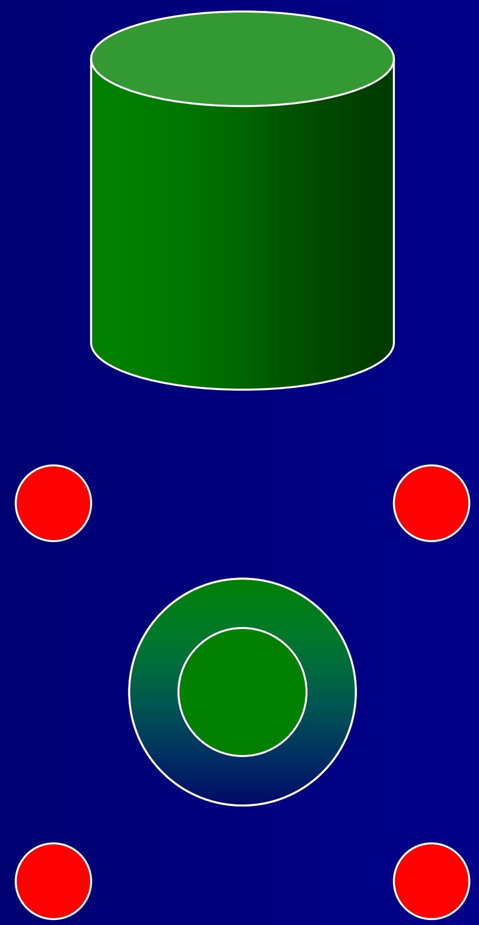

corona

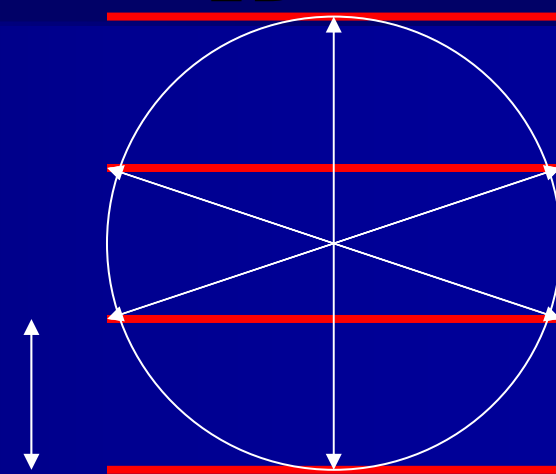

Crystall lattice modulation in YBCO

x-ray diffraction (synchrotron radiation), neutrons

Islam Z. *et al.*, PRB **66** (2002) 92501

Modulated lattice

Super-structures

Described by Bessel functions

Analogy with irradiated JJ

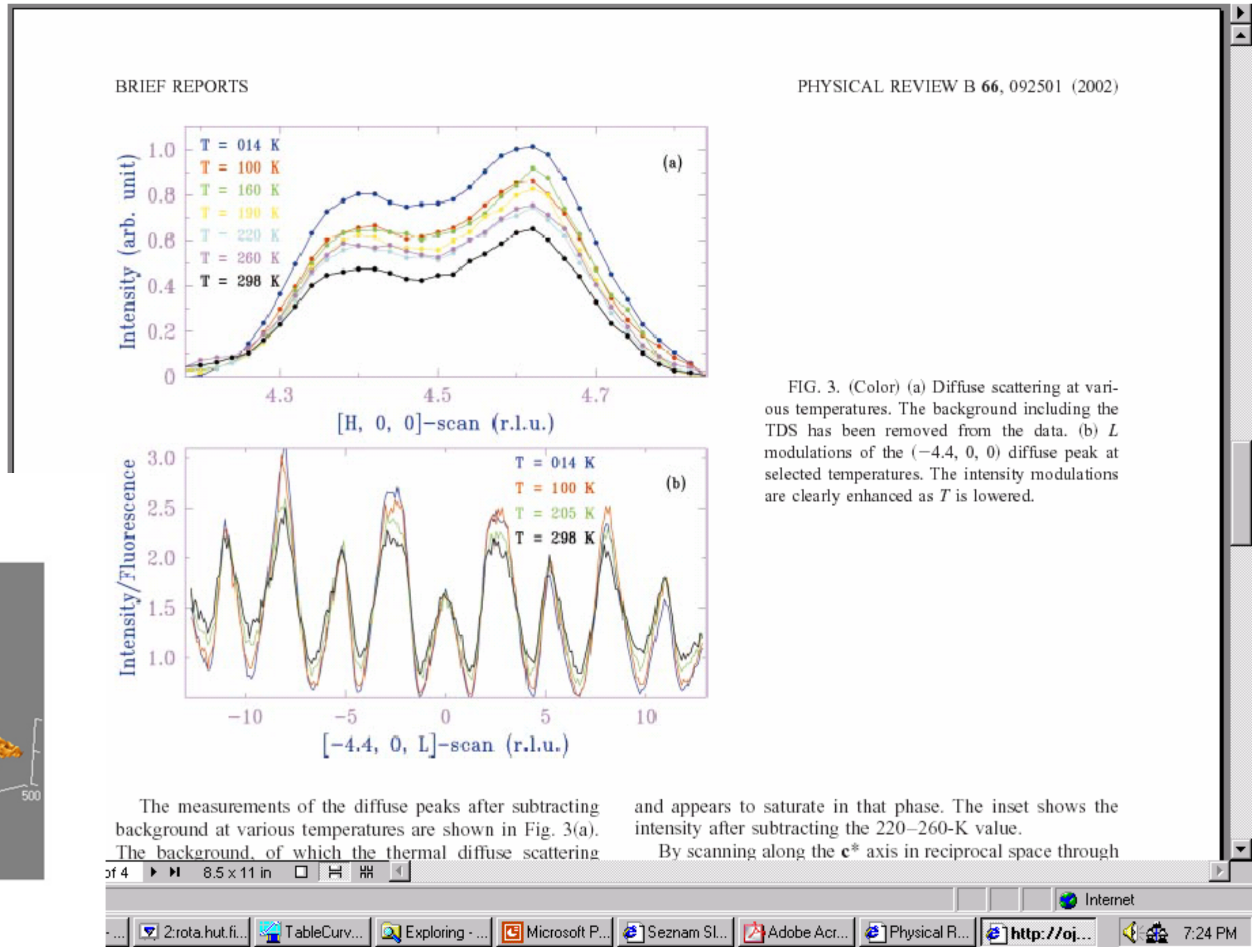
BRIEF REPORTS PHYSICAL REVIEW B **66**, 092501 (2002)

FIG. 3. (Color) (a) Diffuse scattering at various temperatures. The background including the TDS has been removed from the data. (b) L modulations of the (−4.4, 0, 0) diffuse peak at selected temperatures. The intensity modulations are clearly enhanced as T is lowered.

The measurements of the diffuse peaks after subtracting background at various temperatures are shown in Fig. 3(a). The background, of which the thermal diffuse scattering

and appears to saturate in that phase. The inset shows the intensity after subtracting the 220–260-K value.

By scanning along the c^* axis in reciprocal space through

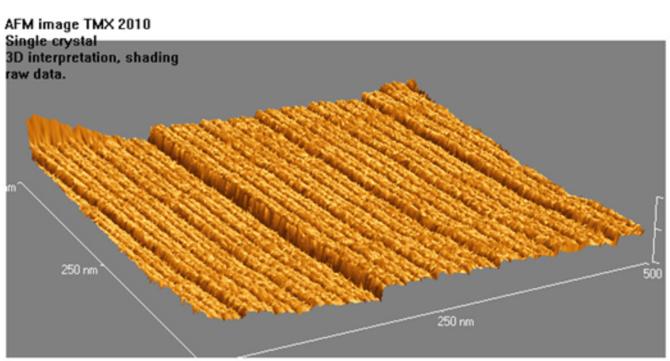

ARPES on Bi2223

Sato T. *et al.*, PRL **89** (2002) 67005

BCS gap is temperature dependent Δ(T)

Pseudogap width is temperature independent (one needs invoke real space gap). There are states within the gap even at 0 K and gap fills with increasing temperature

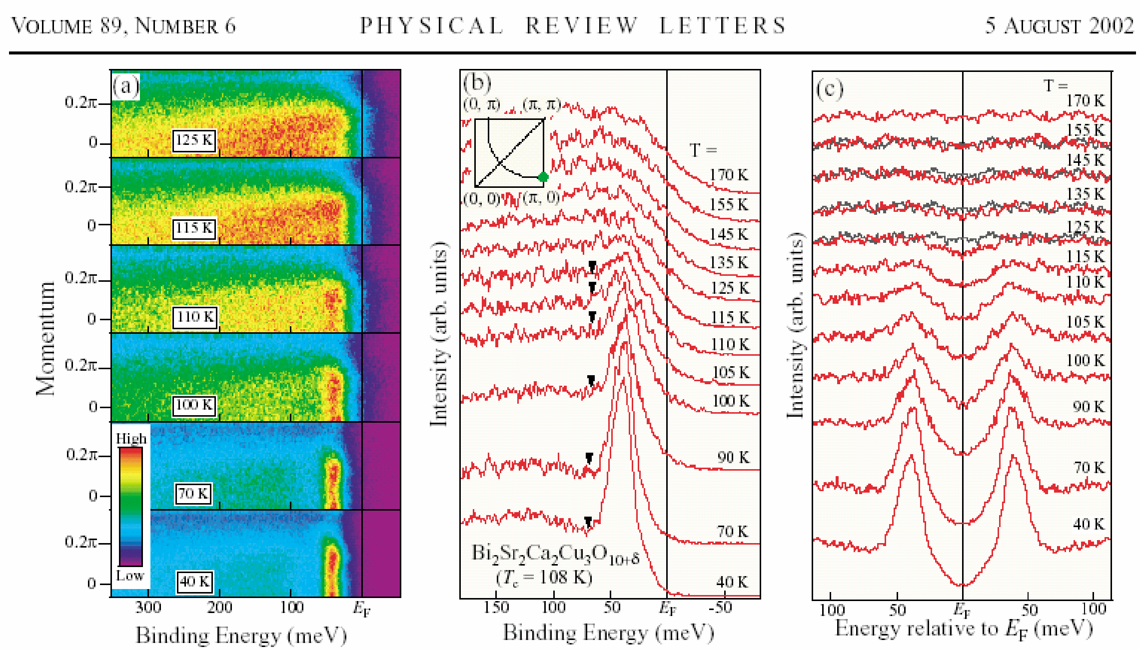
VOLUME 89, NUMBER 6 PHYSICAL REVIEW LETTERS 5 AUGUST 2002

FIG. 3 (color). (a) Temperature dependence of ARPES intensity along $(\pi, 0)$-(π, π) cut in Bi2223. Vertical axis corresponds to the momentum along $(\pi, 0)$-(π, π) cut while the abscissa shows the binding energy relative to E_F. Intensity is normalized to the peak maximum at each temperature. (b) Temperature dependence of ARPES spectra of Bi2223 at $(\pi, 0)$-(π, π) crossing. Intensity of spectra is normalized to the area under the curve. The energy position of spectral break is indicated by arrows. (c) Symmetrized ARPES spectra of Bi2223 at $(\pi, 0)$-(π, π) crossing. The 170-K spectrum (black line) is superimposed on each spectrum for comparison.

[Fig. 3(b)], where a spectral break (indicated by triangles) ... In Fig. 4, we show key superconducting- and pseudogap

ARPES on Bi2212 – Fermi surface

Bogdanov et al., PRL **89** (2002) 167002

1D and 2D Fermi surface

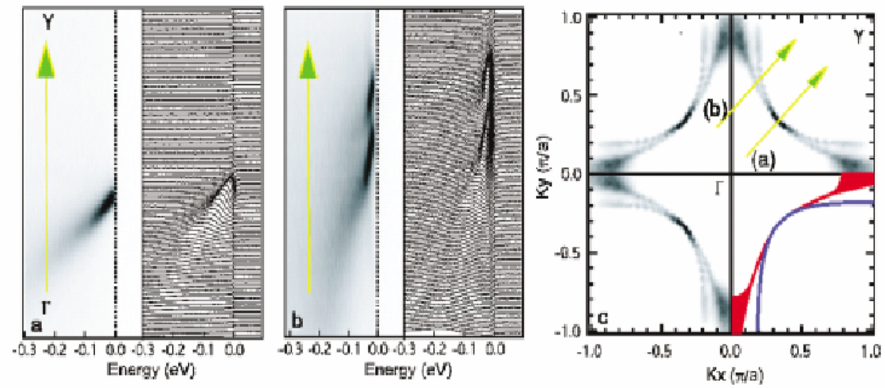

FIG. 1 (color). Panel (a) of this figure shows raw ARPES data along the Γ-*Y* scan. In panel (b), we plot data for the parallel cut 10° off the Γ-*Y* direction. In panel (c), an eightfold symmetrized map of the spectral intensity at 12 meV binding energy in superconducting Bi2212 is presented. This map is representative of the Fermi surface situation in Bi2212. The lower right quadrant of the Brillouin zone in panel (c) identifies the bonding band Fermi surface (blue) and the antibonding band Fermi surface (red).

STM on Bi:2201 – Pseudogap and chains

Kugler M. *et al.*, PRL **86** (2001) 4911

Horizontal, vertical and diagonal stripes (chains)

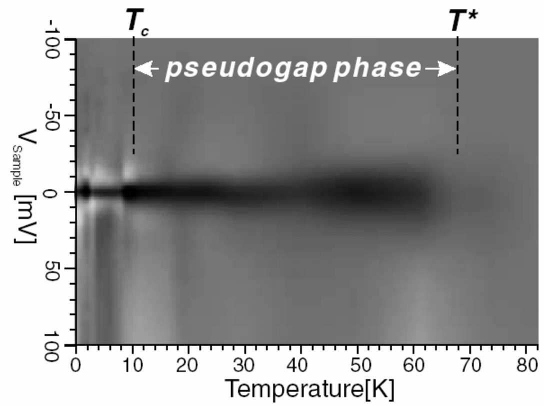

FIG. 4. Interpolated top-view representation of the spectra shown in Fig. 3. The grey scale corresponds to the normalized differential tunneling conductance.

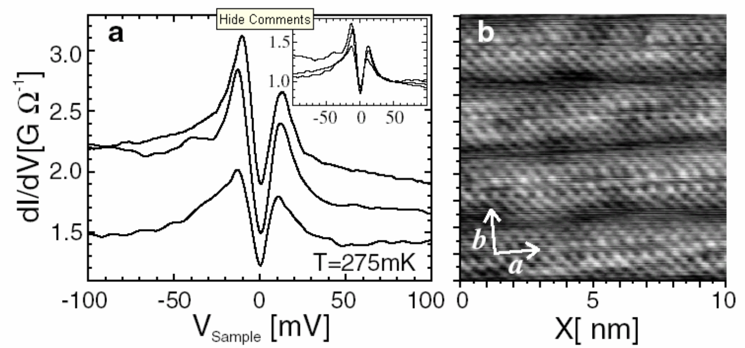

FIG. 1. (a) dI/dV spectra obtained at 275 mK at different locations on *in situ* cleaved Bi2201 ($T_c = 10$ K). In the main panel the spectra are shifted vertically by 0.2 GΩ^{-1} for clarity. In the inset they are superposed and normalized. The peaks are at $\pm\Delta_p = 12$ meV. (b) 10×10 nm^2 constant current image ($R_t = 1.5$ GΩ, raw data) showing atomic resolution and the 26 Å periodic superstructure along the b axis.

Conclusions

- High resolution flux measurements &X-ray&ARPES&STM
- Temperature dependent scattering (el, inel)
- Resonance backscattering
- Real space gap – pseudo-gap
- Low dimensional system
- Ordering/modulation? – spin, charge, orbital

Future directions

- 3x magnetometer with **single vortex resolution**
- Study of low dimensional system
- Resolution $\delta k \sim 10^{-6} k_F$, $\delta E \sim 10^{-6} E_F$ (ARPES has 1 meV)

! Call for materials where $2k_F \sim G$ (structural transitions) high-quality single crystals and epitaxial films

! New field and method – theory needed